Engineering Research Journal
journal homepage: https://erj.journals.ekb.eg/

Digital Measurement and Display of Tractor Longitudinal Wheel Slip Under Various Conditions

Mohamed. Gamal[1], El-Zomor, H. M.[2], S.M Shaaban[3], Mohamed M. Abd elhafiz[3, *]

[1] New Cairo Technological University, Faculty of Industrial and Energy, Autotronics Department, Cairo, Egypt
[2] Arab Academy for Science and Technological, Smart Village, Giza, Egypt
[3] Helwan University, Faculty of Engineering, Automotive and Tractors Department, Cairo, Egypt
*Corresponding Author E-mail: dr.mohamed.hafiz@m-eng.helwan.edu.eg

Abstract.
Longitudinal wheel slip in off-road vehicles negatively impacts tractor traction, leading to power loss, decreased productivity, increased fuel consumption, and accelerated tire wear. By monitoring slip values, drivers can adjust acceleration to optimize vehicle performance, enhancing productivity and mobility. This paper presents the implementation of a microcontroller-based embedded system in 2WD tractors to measure and monitor slip ratio for the driver. Both actual and theoretical tractor speeds were recorded, with results displayed on LCD screens. A warning system alerted the driver when the slip ratio exceeded permissible limits. Field tests were conducted on various terrains (asphalt and sand) at a speed of 15 km/h using different loads (0, 2000, and 4000 N) and varying tire inflation pressures (15/20, 25/30, and 30/40 PSI for rear/front tires). Results on asphalt showed that slip ratio increased from 1% to 5% with higher tire pressure under no external load, and from 0% to 2% at loads of 2000 N and 4000 N. On sand, slip ratio rose from 6% to 10% with no load and from 5% to 8% at the same load levels. A maximum variation of 4% was observed between the measured and indicated speeds from the front sensor and GPS module.

Keywords: Longitudinal tire slip ratio, Microcontroller, Tractors tire, Embedded system, Off-Road Vehicles

1 Introduction

Recently, there has been increased interest in measuring the slip ratio to conserve energy, reduce fuel consumption, and enhance the productivity of equipment used in agriculture, construction, and reclamation. Slip affects the assessment of tractor tractive performance and the effective operation of implements. Tractor slippage is influenced by the specifications of the driving wheels and the physical and mechanical properties of the soil [1]. Slip ratio is a crucial parameter for evaluating wasted energy and traction efficiency. Effective control of the tractor-implement system can reduce exhaust emissions

DOI: 10.21608/erj.2024.306715.1079
Received 27 July 2024; Received in revised form 09 September 2024; Accepted 16 September 2024
Available online 01 December 2024

by up to 10% [2]. Studies have shown that slip and rolling resistance can lead to more than 50% power dissipation, which depletes tires and compacts soil, adversely affecting crop production[3], [4].

According to previous studies, driving wheel slippage should not exceed 16%, as this leads to reduced field performance, increased fuel consumption, and greater soil structure deformation [5], [6]. Agricultural tractors operating off-road are most efficient when drive wheel slippage is between 8-12% [7], [8]. It has been observed that if slippage decreases to 5-7%, energy consumption per unit of work actually increases due to suboptimal traction power utilization [9], [10]. Tillage depth and forward speed play a significant role in determining slippage in off-road vehicles [11]. Studies have demonstrated that increased slippage leads to higher fuel consumption and decreased field capacity performance under various field conditions [12].

Tractors are essential machines for driving field operations in agriculture. Fuel consumption for tractors depends on traction power and power loss [13]. Agricultural wheeled machines, particularly tractors, consume substantial energy due to the complex interaction between the topsoil and tires, leading to stochastic tire deflection and soil deformation. Research shows that 20-55% of available tractor power is lost during the tire-soil interaction. Reducing tire inflation from 180 kPa to 65 kPa or 75 kPa for wide, low-profile tires increased the front tire footprint by 24.7% and the rear tire footprint by 31.1% [14].

Power loss directly affects fuel consumption, which in turn contributes to greenhouse gas emissions [15]. Therefore, it is crucial to focus on minimizing energy loss and maximizing energy efficiency in agricultural tractors. Key factors influencing drive wheel performance include vertical wheel loads, tire inflation pressures, and wheel slip [4], [5], [16], [17]. It has been observed that reducing tire pressure improves traction coefficient, power delivery efficiency, and fuel consumption, while increasing wheel vertical load primarily reduces fuel consumption[5]. However, low tire pressure does not always guarantee better drawbar characteristics [16].

The vertical load and tire inflation pressure are critical for footprint area, which can indicate tire/road interaction conditions such as stiffness, loading capability, and terrain bearing capacity. Adjusting inflation pressure and power can help minimize tire energy loss. At flotation pressure, tire deformation matches soil sinking without slippage, achieving off-road vehicle mission objectives[18]–[20].

Most agricultural tractors feature all-wheel (four-wheel) drive, enhancing pull with less slip by utilizing the full weight of the machine for grip. However, on dry roads, energy is often wasted on driving the front axle. To leverage the benefits of four-wheel drive and reduce wheel slip ratio, a system for monitoring longitudinal wheel slip ratio has been implemented to control vehicle driving and optimize slip ratio factors [21]–[23].

.

Previous research emphasizes the importance of the rear wheel slip ratio, as it influences tire wear, fuel efficiency, productivity, and soil compaction. Studies have identified that the ideal slip ratio for tractor wheels is between 8% and 15%, as maintaining this range improves power efficiency.

2 Methodology

The following section will provide a brief explanation of the mechanical equipment, electronic devices, and tools used.

2.1 Tractor Specifications

In off-road applications, various types of tractors are employed on agricultural lands for plowing or harrowing the soil and transporting crops via highways. Heavy equipment is also used to compact and prepare the soil for asphalting. In this study, a commonly used tractor for agricultural and sandy terrains was selected.

A Belarus rear-wheel-drive (2WD) tractor, as shown in Fig. 1, was used for this research. Table 1 provides the tractor's technical specifications.

Table 1 The Tractor Specifications

Make	Belarus
Model	925
Production years	1995
Fuel	Diesel
Front tires dimensions	11.2-20
Rear tires dimensions	16.9-38
Engine size	4.7 L
Number of cylinders	4 Cylinders
Horsepower	100 Hp
Fuel tank capacity	129.8 L
Compression ratio	16:1
Transmission gears	18 Forward and 4 Reverse

Fig. 1 The Tested 2WD Tractor

2.2 Field Site Specifications

Field tests were conducted at two sites in Qena Governorate, Egypt, located at (26°01'16.7"N, 32°07'32.9"E) and (26°01'03.3"N, 32°07'28.2"E). These sites feature different soil textures and conditions. The first location, with sandy soil, represents an Off-Road terrain; the second location, an asphalt highway, serves as an example of on-road terrain (see Fig. 2).

Fig. 2 Terrain Location (a) on road (Asphalt) (b) off road (Sand)

2.3 Soil descriptions.

The cone index (CI) is a key indicator of soil strength and, along with its gradient relative to penetration depth, is used to simulate the capability of off-road vehicles on a given terrain. CI readings were obtained using a penetrometer according to ASABE S313.2 standards, with a conical base area of 0.130 cm² and an angle of 30º. Measurements were taken at depths ranging from 1 to 6 inches, in 1-inch increments, across several areas of the field. The CI results, shown in Table 2, indicate the mean CI for three sites as 85.71, 79.29, and 88 lbf. The pressure-sinkage relationship for these locations is illustrated in Table 3 and Fig. 3.

Table 2 Mean Soil Cone Index

	Cone Index (CI), Ibf		
	CI_1	**CI_2**	**CI_3**
Average Cone Index (CI)	85.71	79.29	88.57
	= (CI_1 + CI_2 + CI_3 / 3) = 84.52		

Table 3 Relationship between pressure-sinkage for three locations

Sinkage (Inch)	***Pressure (Ibf)***		
	Location 1	**Location 2**	**Location 3**
0	0	0	0
1	15	20	20
2	25	45	60
3	60	70	105
4	135	110	125
5	180	145	145
6	185	165	165

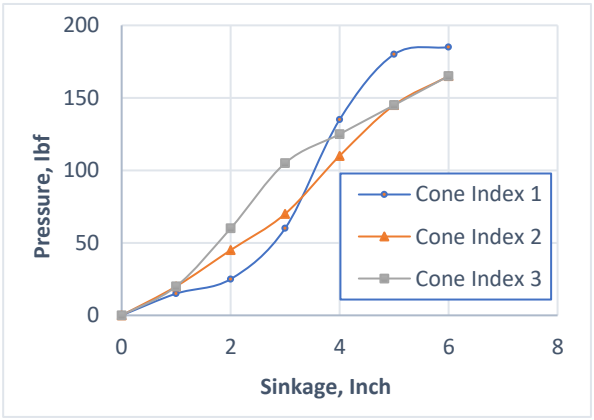

Fig. 3 Pressure-Sinkage relationship for three locations

Laboratory Test for Soil Analysis. A sieve analysis test has been conducted as shown in Fig.4 to analyze the sand soil properties that were used in the field test. The steps of the experiment were according to, and the results of the soil analysis were as follows in Fig.5.

2.4 Measurement Sensors Calibration

The sensors were calibrated by setting specific travel distances and speeds, as shown in Fig. 5. The theoretical number of wheel revolutions was calculated based on the circumference of the tractor tire and compared with the actual revolutions measured by the Hall effect sensors, as shown in Fig. 6. The calibration results indicated that the error rate did not exceed 3.71% when comparing the theoretical wheel revolutions to those recorded by the sensors, as illustrated in Fig. 7.

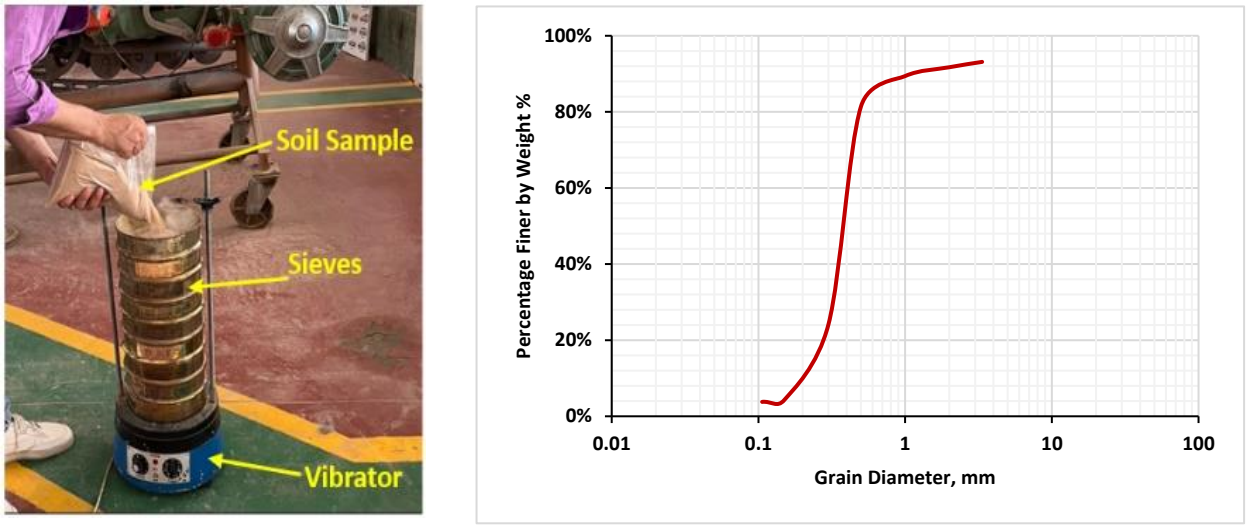

Fig. 4 Grain size distribution test method and results

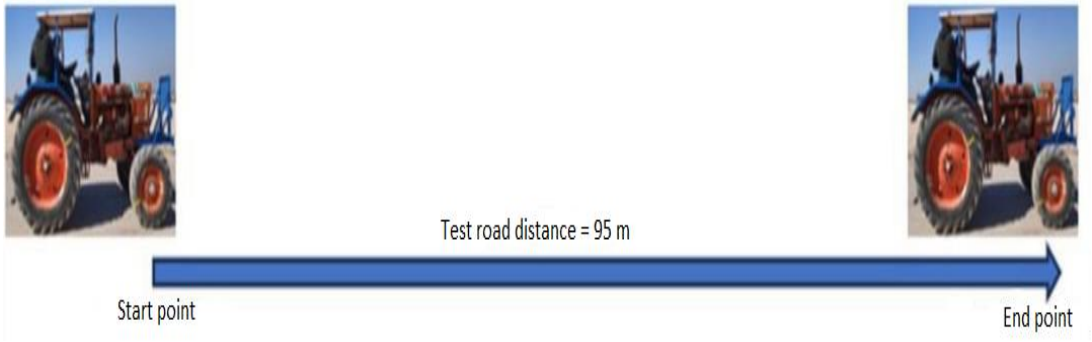

Fig. 5 Illustration of the calibration process

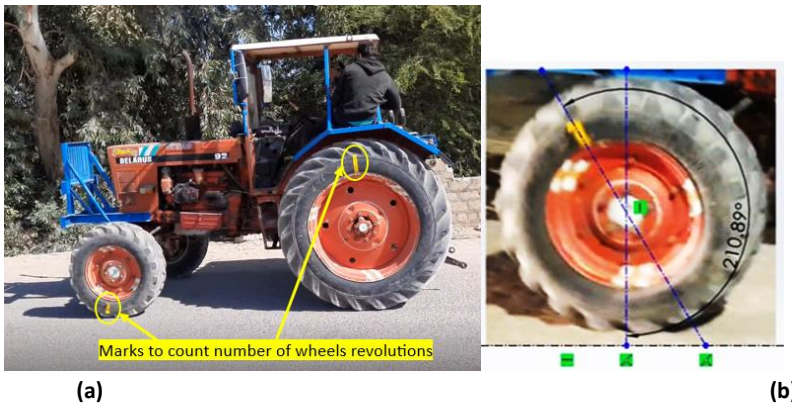

Fig. 6 Illustration of the calibration process of the tractor in motion

Additionally, the GPS module was calibrated by operating the tractor at both slow and fast speeds within its range, from 5 to 15 km/hr. The comparison between the GPS readings and the sensor measurements for tractor speed revealed an error rate of 4.13%, as detailed in Fig. 8.

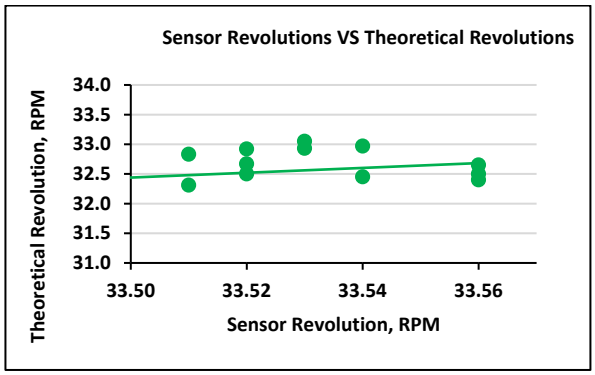

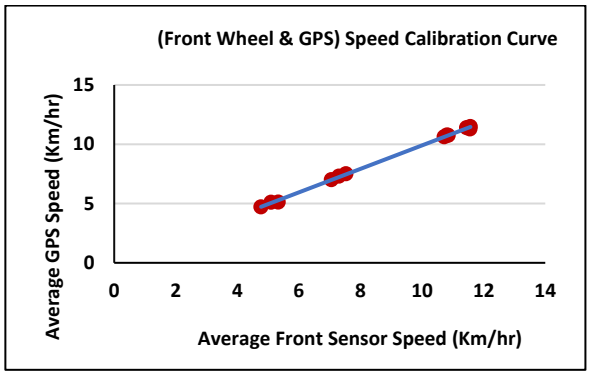

Fig. 7 Sensor and Theoretical Revolutions Calibration Fig. 8 Front Wheel and GPS Speeds Calibration

2.5 Field Test

Tire Slip Measuring and Monitoring System: Tire Slip Measurement and Monitoring System: The tractor under test is illustrated in Fig. 9. The longitudinal slip ratio is determined by comparing the actual and theoretical speeds of the tractor. The theoretical speed is calculated based on the average RPM of the rear wheels, while the actual speed is assessed from the front wheels [24]. Additionally, to validate the wheel slip ratio, the actual speed was also measured using a GPS module.

Fig. 9 Overall view of installed sensors with tractor

To measure the angular speed of the front and rear wheels, two Hall effect sensors and magnets were employed, as depicted in Fig. 10. These measurements were then used to calculate the wheel slip ratio, as detailed in the following equations.

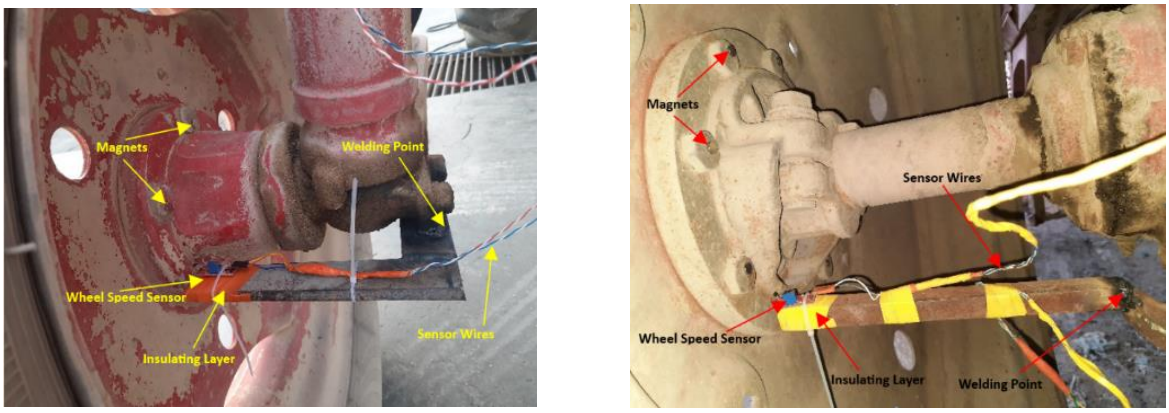

(a) **(b)**

Fig. 10 Hall effect sensors and magnets installation on rear wheel and front wheel, **a)** Rear wheel b) Front wheel

$$S_{th} = N \times D \times \text{Const.} \quad (1)$$

$$S_r = (N_1 \times D_1 \times 0.001885) \quad (2)$$

$$S_f = (N_2 \times D_2 \times 0.001885) \quad (3)$$

$$S_{R1} = (S_r - S_f) \quad (4)$$

$$S_R = (S_{R1} / S_r) * 100 \quad (5)$$

S_{th}: Theoretical Speed, km/hr
S_r, S_f: Rear and Front Wheel Speed, km/hr
N_1, N_2: Rear and Front Wheel Revolutions
D, D_1 and D_2: Rear and Front Wheel Diameter, cm
Constant = $[(\pi \times 3600)/ (60 \times 100 \times 1000)]$
S_{R1}: Difference between Rear and Front Wheel Speed
S_R: Longitudinal Slip %

The GPS module was employed to track the tractor's location and continuously update its speed. The wheel slip ratio was assessed by comparing the pulses received from the sensors to predefined slip ratio ranges. The microcontroller's computer interface allows for the setting of a recommended slip ratio value. Based on previous research, a range of permissible slip ratios was established. If the slip ratio falls below the lower limit or exceeds the upper limit, the microcontroller triggers a buzzer and indicator LED to alert the driver that the slip ratio limits have been breached. If the slip ratio remains within the acceptable range, no action is taken by the system. Additionally, tire inflation pressure was monitored during the experiment using an external pressure gauge.

Slip Measurement Instrumentation. Fig. 11 presents the complete wiring layout for two developed systems designed to measure and monitor the slip ratio. The layout illustrates the sensors and their connections to the main circuit components. In the first system, the theoretical tractor speed is derived from the rear wheel, while the actual speed is measured from the front wheel, as shown in Fig. 11a. In the second system, the theoretical tractor speed is also obtained from the rear wheel, but the actual speed is measured using the GPS module, as depicted in Fig. 11b.

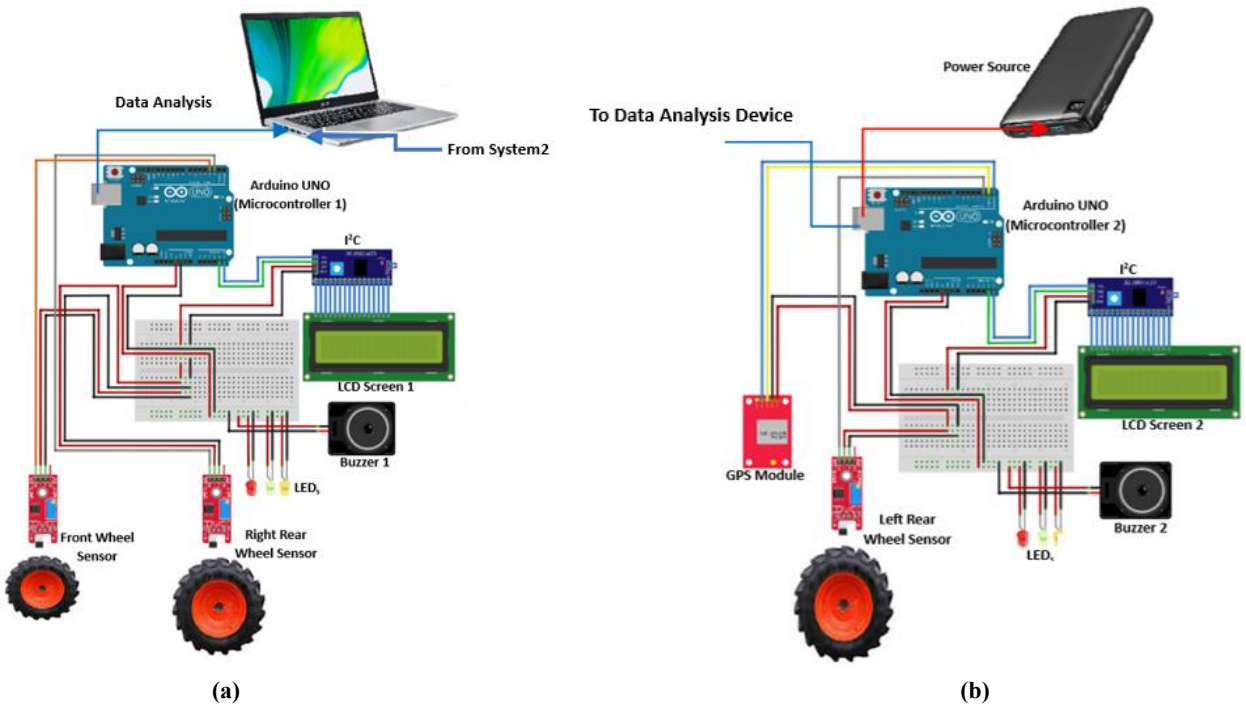

Fig. 11 A complete layout of System a & b

One of the three Hall Effect sensors was mounted on the front wheel of the tractor, while the other two were mounted on the rear wheels. Magnets were attached to the rims of both the front and rear wheels. Each time a sensor passed by a magnet; it generated a voltage signal pulse. The total number of pulses in a single revolution corresponded to the number of magnets mounted on the tractor wheels. These signal pulses were recorded by the microcontroller, where an integrated development environment (IDE) algorithm calculated the tractor's actual and theoretical speeds. A GPS module, located in the driver's compartment, measured the actual speed of the tractor and compared it with the theoretical speed derived from the rear wheel speed sensor. The system then calculated the slip ratio and displayed it on the LCD screen in front of the driver, providing real-time feedback on the tractor's condition while driving, as shown in Fig. 12.

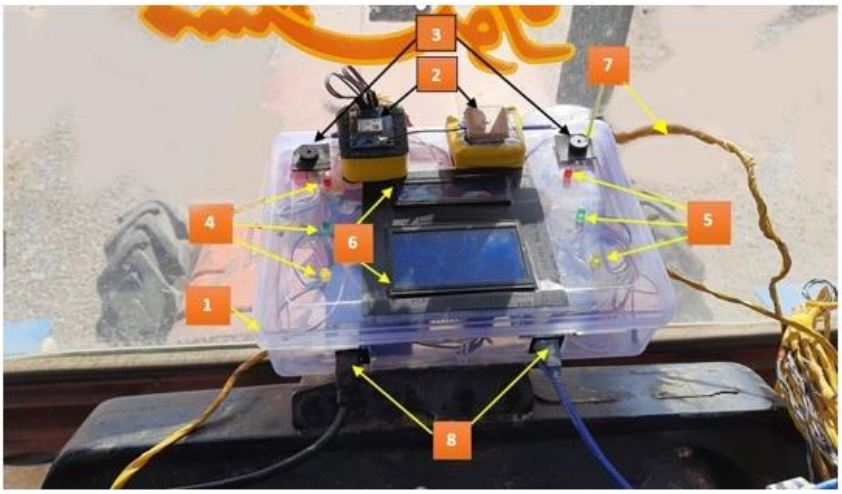

1- Housing
2- GPS Module& Antenna
3- Buzzer for System 1 &2
4- LED_s for System 1
5- LED_s for System 2
6- LCD Screen for System 1 &2
7- Wires from Sensors
8- Power Supply and Data Cables

Fig. 12 Overall view of developed slip indicating device

To alert the driver when the slip ratio exceeds the permissible limit, a warning system with three LEDs (green, yellow, red) and a buzzer is provided. As shown in the flowchart in Fig. 13, the green LED remains lit continuously, indicating that the system is operating within the optimal range of 8% to 15%. When the slip ratio falls below 8%, the yellow LED lights up, and if the slip ratio exceeds 15%, the red LED illuminates, accompanied by the activation of the buzzer to warn the driver."

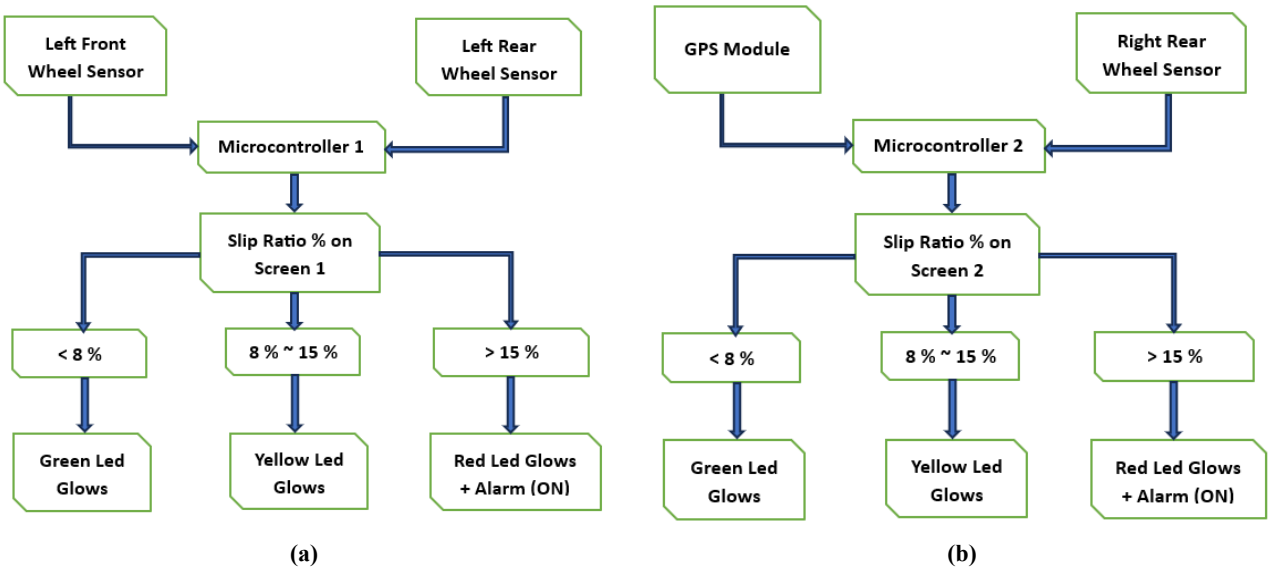

Fig. 13 Flow chart of the developed system

3 Results And Discussion

Outliers were removed, and mean values were calculated for each slip range. Traction tests were conducted in steady-state motion to measure the slip ratio of tractor tires under varying conditions, including two types of terrain, different tractor speeds, loads, and tire inflation pressures.

3.1 Sandy Soil Results

The slip ratio of the tractor tires on sandy soil was measured without any external load. The rear tires were inflated to 15 psi and the front tires to 20 psi, with the tractor moving at a speed of 15 km/h.

The tire pressures were then adjusted to 25 psi for the rear and 30 psi for the front, and the experiment was repeated three times under the same conditions. Afterward, the tire pressures were further increased to 30 psi for the rear and 40 psi for the front, maintaining the same speed of 15 km/h, with no external load.

Next, a 2000 N external load was applied to the tractor, and the rear tire pressures were adjusted to 15, 25, and 30 psi, with corresponding front tire pressures of 20, 30, and 40 psi, respectively, while maintaining a speed of 15 km/h. The load was then increased to 4000 N, and the same tests were repeated on sandy terrain with the same tire pressure configurations.

The results showed that as tire pressure increases, the slip ratio also increases due to the smaller contact area between the tires and the ground. Conversely, the slip ratio decreases with lower tire pressure, as the larger contact area improves traction with the ground, reducing slippage (Fig. 16-18).

Fig.s 19-21 demonstrate that as external load increases, the slip ratio decreases because the increased weight enhances tire grip and contact with the ground. In contrast, when the external load decreases, the slip ratio increases due to reduced grip and contact area.

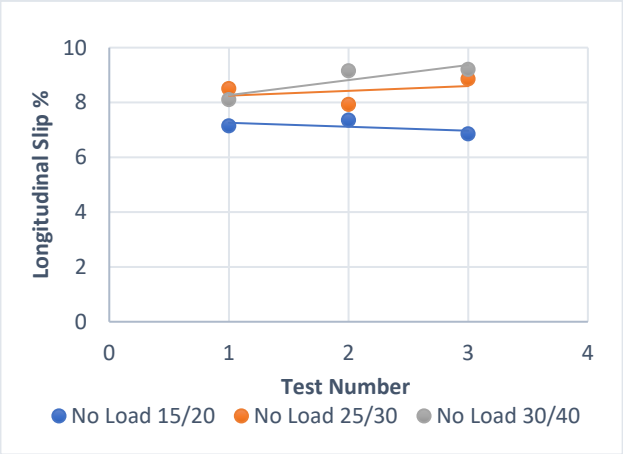

Fig.14 Longitudinal Slip Vs Inflation Pressure at No External Load

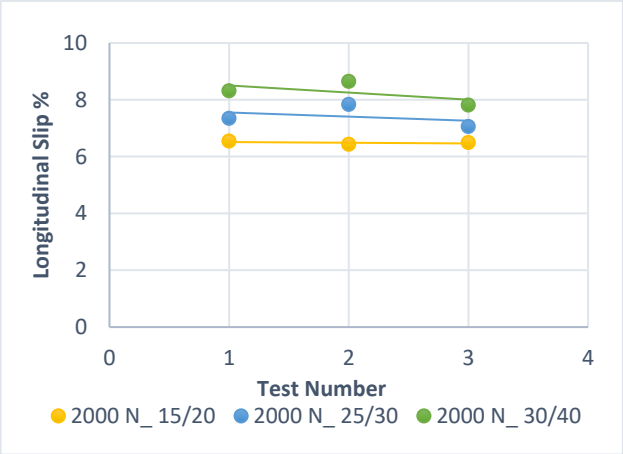

Fig.15 Longitudinal Slip Vs Inflation Pressure at Load 2000 N

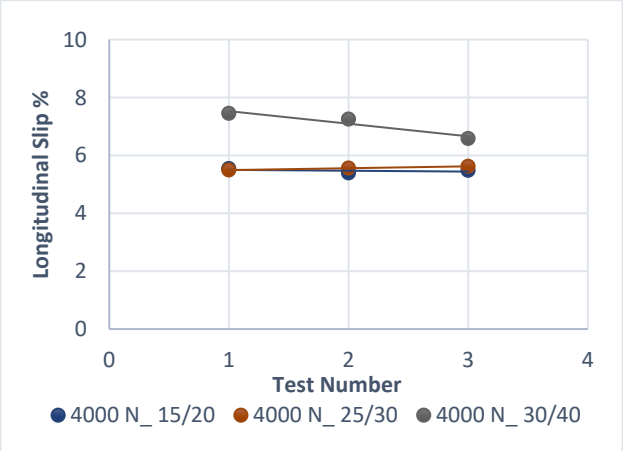

Fig.16 Longitudinal Slip Vs Inflation Pressure at Load 4000 N

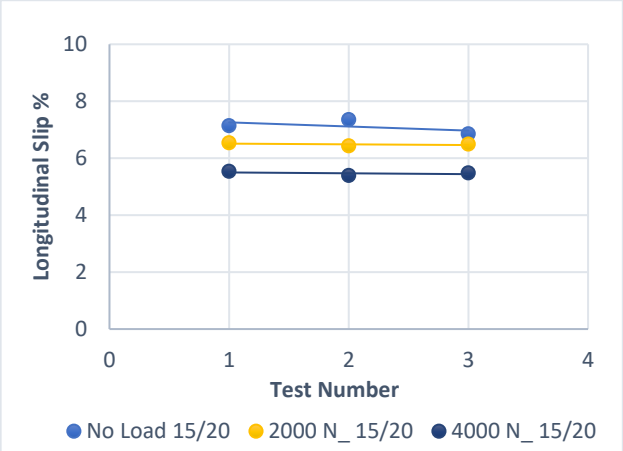

Fig.17 Longitudinal Slip Vs Different Load at Inflation Pressure (15/20) Psi

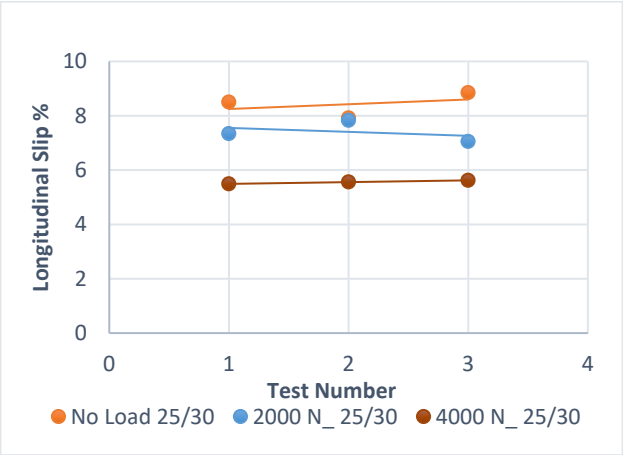

Fig.18 Longitudinal Slip Vs Different Load at Inflation Pressure (25/30) Psi

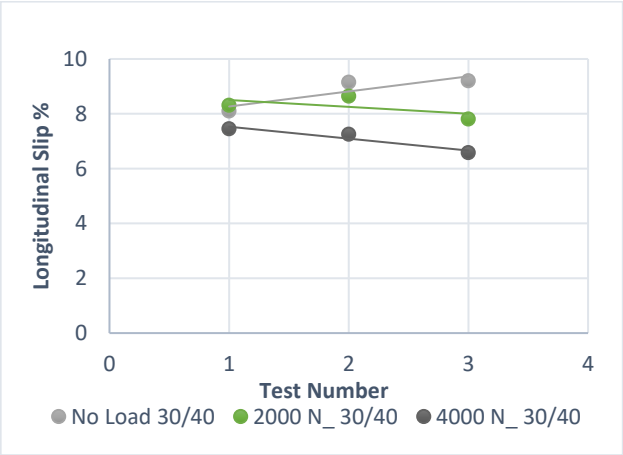

Fig.19 Longitudinal Slip Vs Different Load at Inflation Pressure (30/40) Psi

3.2 Asphalt Road Results

The tractor was evaluated on asphalt terrain without external load, starting with tire pressures of 15 psi for the rear tires and 20 psi for the front tires, at a speed of 15 km/h. The tire pressures were then adjusted to 25 psi for the rear and 30 psi for the front, with the tractor continuing to drive on asphalt at 15 km/h. Subsequently, the tire pressures were increased to 30 psi for the rear tires and 40 psi for the front tires, maintaining the same speed of 15 km/h on asphalt without any external load.

Next, a 2000 N external load was applied, and the tests were repeated on asphalt with rear tire pressures set to 15, 25, and 30 psi, and corresponding front tire pressures of 20, 30, and 40 psi, respectively. Finally, the external load was increased to 4000 N, and the tests were conducted again under the same tire pressure configurations at the same speed.

Fig.20 Longitudinal Slip Vs Inflation Pressure at No External Load

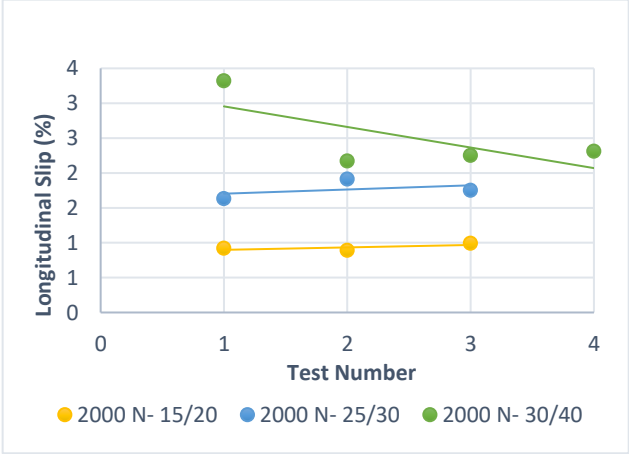

Fig.21 Longitudinal Slip Vs Inflation Pressure at Load 2000 N

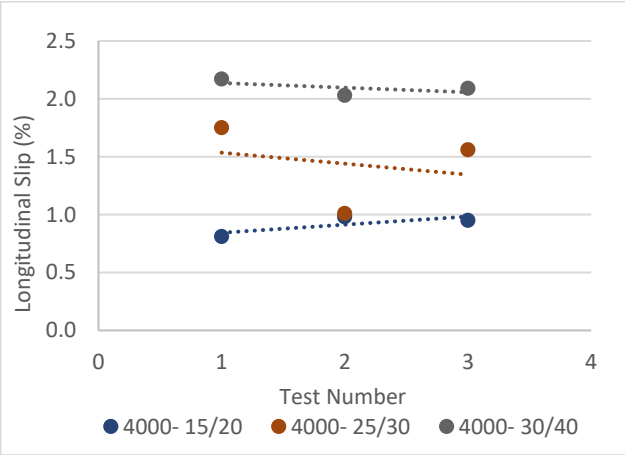

Fig.22 Longitudinal Slip Vs Inflation Pressure at Load 4000 N

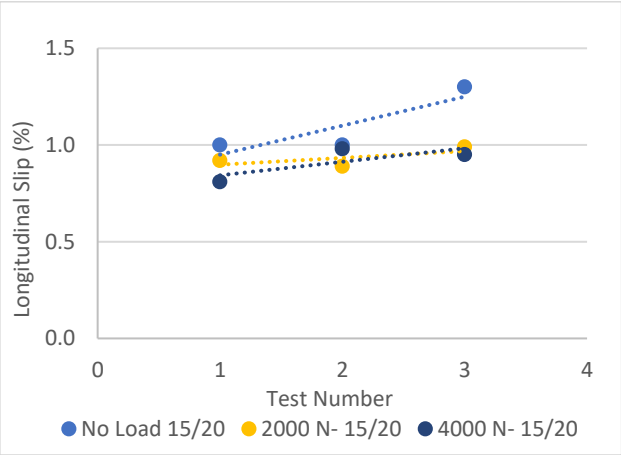

Fig.23 Longitudinal Slip Vs Different Load at Inflation Pressure (15/20) Psi

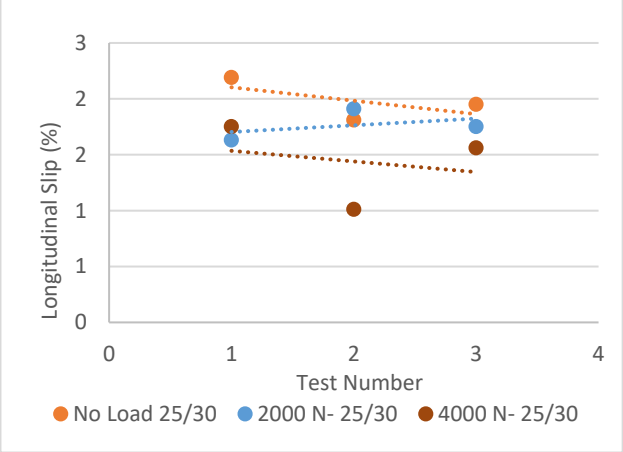

Fig.24 Longitudinal Slip Vs Different Load at Inflation Pressure (25/30) Psi

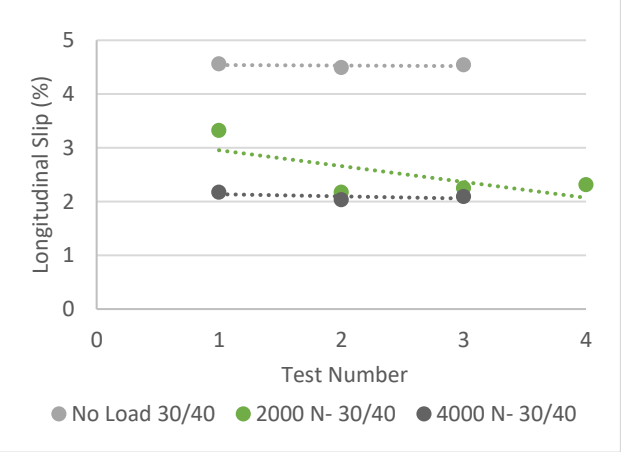

Fig.25 Longitudinal Slip Vs Different Load at Inflation Pressure (30/40) Psi

The results showed that the slip ratio increases with higher tire pressure, likely due to the smaller contact area between the tire and the ground. Conversely, the slip ratio decreases as tire pressure is reduced, as the larger contact area improves grip, reducing slippage (Fig. 20-22). Additionally, as the external load increases, the slip ratio decreases due to the enhanced grip and increased contact area between the tires and the ground. Conversely, when the external load decreases, the slip ratio increases due to reduced grip and contact area, as illustrated in Fig.s 23-25.

Also, the results demonstrated that the slip ratio increases as ground cohesion decreases, such as on sandy terrain, and decreases as ground cohesion increases, such as on asphalt. This occurs because less cohesive surfaces are less capable of resisting the traction forces generated by the moving vehicle. As shown in Fig. 26, the differences in slip ratio between on-road and off-road conditions at various tire pressures and a tractor speed of 15 km/h are evident.

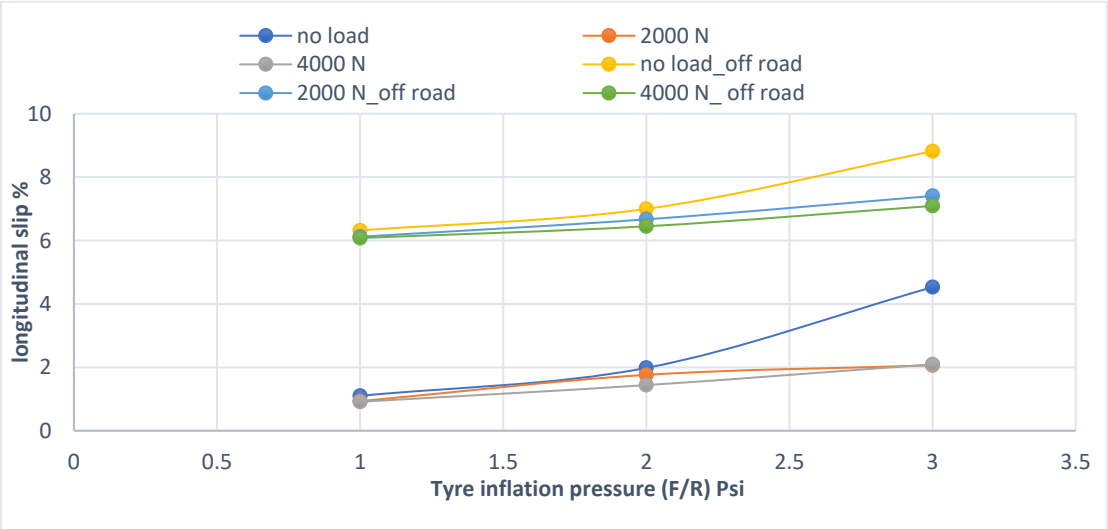

Fig.26 Longitudinal Slip Vs Different Load at Inflation Pressure (25/30) Psi

4 Conclusion

The results, obtained on both asphalt and sandy soil at a vehicle speed of 15 km/h with tire pressures of 15/20, 25/30, and 30/40 psi for the rear/front tires respectively, and with no external load, 2000 N, and 4000 N, revealed the following:

- Both systems used to measure and display the slip ratio produced very accurate results and showed nearly identical performance.
- The system utilizing the GPS module is significantly more expensive, potentially costing up to twice as much as the system using Hall effect sensors.
- The slip ratio increases with higher tire pressure and decreases with lower tire pressure. This is because higher tire pressure reduces the contact area with the ground, stiffens the tire structure, and minimizes tire deformation.
- The slip ratio decreases as external load increases and increases as external load decreases. Lower external load reduces the contact area between the tires and the ground, leading to a lower normal force and traction force.
- The slip ratio rises as ground adhesion decreases and falls as adhesion increases, with less adhesive surfaces being less capable of resisting the traction forces generated by the vehicle.
- On asphalt, the slip ratio ranges from 1% to 5%, while on sand it ranges from 6% to 9%, as tire pressure increases and external load decreases.
- A maximum variation of 4% was observed between the measured speeds using the front Hall effect sensor and the GPS module.

References

[1] S. A. Almaliki, M. S. Himoud, and S. J. Muhsin, “Mathematical model for evaluating slippage of tractor under various field conditions,” *Basrah J. Agric. Sci.*, 2021, doi: 10.37077/25200860.2021.34.1.05.

[2] S. H. Karparvarfard and H. Rahmanian-Koushkaki, “Development of a fuel consumption equation: Test case for a tractor chisel-ploughing in a clay loam soil,” *Biosyst. Eng.*, 2015, doi: 10.1016/j.biosystemseng.2014.11.015.

[3] A. Ashok Kumar, V. K. Tewari, C. Gupta, and C. M. Pareek, “A device to measure wheel slip to improve the fuel efficiency of off road vehicles,” *J. Terramechanics*, 2017, doi: 10.1016/j.jterra.2016.11.002.

[4] H. Taghavifar, A. Mardani, and H. Karim-Maslak, “Multi-criteria optimization model to investigate the energy waste of off-road vehicles utilizing soil bin facility,” *Energy*, 2014, doi: 10.1016/j.energy.2014.06.081.

[5] A. Battiato and E. Diserens, “Influence of Tyre Inflation Pressure and Wheel Load on the Traction Performance of a 65 kW MFWD Tractor on a Cohesive Soil,” *J. Agric. Sci.*, 2013, doi: 10.5539/jas.v5n8p197.

[6] V. Damanauskas, A. Janulevicius, and G. Pupinis, “Influence of Extra Weight and Tire Pressure on Fuel Consumption at Normal Tractor Slippage,” *J. Agric. Sci.*, 2015, doi: 10.5539/jas.v7n2p55.

[7] A. Battiato and E. Diserens, “Tractor traction performance simulation on differently textured soils and validation: A basic study to make traction and energy requirements accessible to the practice,” *Soil Tillage Res.*, 2017, doi: 10.1016/j.still.2016.09.005.

[8] J. W. Lee, J. S. Kim, and K. U. Kim, “Computer simulations to maximise fuel efficiency and work performance of agricultural tractors in rotovating and ploughing operations,” *Biosyst. Eng.*, 2016, doi: 10.1016/j.biosystemseng.2015.11.012.

[9] “Theory of ground vehicles,” *Proc. Inst. Mech. Eng. Part D J. Automob. Eng.*, vol. 216, no. 7, pp. 629–629, Jul. 2002, doi: 10.1243/095440702760178640.

[10] J. Y. Wong, *Theory of Ground Vehicles*. 2022.

[11] S. M. Shafaei, M. Loghavi, and S. Kamgar, “Feasibility of implementation of intelligent simulation configurations based on data mining methodologies for prediction of tractor wheel slip,” *Inf. Process. Agric.*, 2019, doi: 10.1016/j.inpa.2018.10.004.

[12] G. Moitzi *et al.*, “Effects of working depth and wheel slip on fuel consumption of selected tillage implements,” *Agric. Eng. Int. CIGR J.*, 2014.

[13] J. O. Peça *et al.*, “Speed advice for power efficient drawbar work,” *J. Terramechanics*, 2010, doi: 10.1016/j.jterra.2009.07.003.

[14] T. Šmerda and J. Čupera, “Tire inflation and its influence on drawbar characteristics and performance - Energetic indicators of a tractor set,” *J. Terramechanics*, 2010, doi: 10.1016/j.jterra.2010.02.005.

[15] V. Van Linden and L. Herman, “A fuel consumption model for off-road use of mobile machinery in agriculture,” *Energy*, 2014, doi: 10.1016/j.energy.2014.09.074.

[16] J. H. Lee and K. Gard, “Vehicle-soil interaction: Testing, modeling, calibration and validation,” *J. Terramechanics*, 2014, doi: 10.1016/j.jterra.2013.12.001.

[17] H. Taghavifar and A. Mardani, “Investigating the effect of velocity, inflation pressure, and vertical load on rolling resistance of a radial ply tire,” *J. Terramechanics*, 2013, doi: 10.1016/j.jterra.2013.01.005.

[18] M. A. A. Emam, S. M. Shaaban, S. M. El-Demerdash, and H. M. El-Zomor, “A computerized tyre pressure control system for off-road vehicles,” *Int. J. Veh. Struct. Syst.*, 2011, doi: 10.4273/ijvss.3.4.01.

[19] H. M. El-Zomor, “Real-time estimation of pneumatic tyre hysteresis loss,” *Int. J. Heavy Veh. Syst.*, 2019, doi: 10.1504/IJHVS.2019.098275.

[20] M. Adel Mohamed, S. Elhussieny, M. A. Emam, and M. M. Abd Elhafiz, “Tire-Soil Interaction Simulation Using Finite Element Method to Investigate Their Deformation and Sinkage,” in *SAE Technical Papers*, 2023, doi: 10.4271/2023-01-5001.

[21] J. Zebrowski, “Traction efficiency of a wheeled tractor in construction operations,” *Automation in Construction*. 2010, doi: 10.1016/j.autcon.2009.09.007.

[22] M. M. Abd El-Hafiz, M. A. A. Emam, W. A. H. Oraby, and S. Shaaban, “Axle torque distribution control for enhancing mobility of off-road vehicles,” *Int. J. Heavy Veh. Syst.*, vol. 21, no. 3, 2014, doi: 10.1504/IJHVS.2014.066080.

[23] M. M. Abd El-Hafiz, M. A. A. Emam, W. A. H. Oraby, and S. Shaaban, “Modeling and simulation of off-road vehicle mobility with driving torque distribution control on split adhesion conditions,” *Int. J. Veh. Struct. Syst.*, vol. 9, no. 2, 2017, doi: 10.4273/ijvss.9.2.07.

[24] A. A. Kumar, V. K. Tewari, and B. Nare, “Embedded digital draft force and wheel slip indicator for tillage research,” *Comput. Electron. Agric.*, 2016, doi: 10.1016/j.compag.2016.05.010.